AMERICAN SOCIETY FOR MICROBIOLOGY | Journal of Bacteriology®

RESEARCH ARTICLE

Two Different Quinohemoprotein Amine Dehydrogenases Initiate Anaerobic Degradation of Aromatic Amines in *Aromatoleum aromaticum* EbN1

Georg Schmitt,[a] Martin Saft,[a] Fabian Arndt,[a] Jörg Kahnt,[b] Johann Heider[a,c]

[a]Laboratory for Microbial Biochemistry, Philipps University of Marburg, Marburg, Germany
[b]Max Planck Institute for Terrestrial Microbiology, Marburg, Germany
[c]LOEWE-Center for Synthetic Microbiology, Marburg, Germany

ABSTRACT Aromatic amines like 2-phenylethylamine (2-PEA) and benzylamine (BAm) have been identified as novel growth substrates of the betaproteobacterium *Aromatoleum aromaticum* EbN1, which degrades a wide variety of aromatic compounds in the absence of oxygen under denitrifying growth conditions. The catabolic pathway of these amines was identified, starting with their oxidative deamination to the corresponding aldehydes, which are then further degraded via the enzymes of the phenylalanine or benzyl alcohol metabolic pathways. Two different periplasmic quinohemoprotein amine dehydrogenases involved in 2-PEA or BAm metabolism were identified and characterized. Both enzymes consist of three subunits, contain two heme *c* cofactors in their α-subunits, and exhibit extensive processing of their γ-subunits, generating four intramolecular thioether bonds and a cysteine tryptophylquinone (CTQ) cofactor. One of the enzymes was present in cells grown with 2-PEA or other substrates, showed an $\alpha_2\beta_2\gamma_2$ composition, and had a rather broad substrate spectrum, which included 2-PEA, BAm, tyramine, and 1-butylamine. In contrast, the other enzyme was specifically induced in BAm-grown cells, showing an $\alpha\beta\gamma$ composition and activity only with BAm and 2-PEA. Since the former enzyme showed the highest catalytic efficiency with 2-PEA and the latter with BAm, they were designated 2-PEADH and benzylamine dehydrogenase (BAmDH). The catalytic properties and inhibition patterns of 2-PEADH and BAmDH showed considerable differences and were compared to previously characterized quinohemoproteins of the same enzyme family.

IMPORTANCE The known substrate spectrum of *A. aromaticum* EbN1 is expanded toward aromatic amines, which are metabolized as sole substrates coupled to denitrification. The characterization of the two quinohemoprotein isoenzymes involved in degrading either 2-PEA or BAm expands the knowledge of this enzyme family and establishes for the first time that the necessary maturation of their quinoid CTQ cofactors does not require the presence of molecular oxygen. Moreover, the study revealed a highly interesting regulatory phenomenon, suggesting that growth with BAm leads to a complete replacement of 2-PEADH by BAmDH, which has considerably different catalytic and inhibition properties.

KEYWORDS 2-phenylethylamine, *Aromatoleum*, adaptation, amine dehydrogenase, anaerobic metabolism, benzylamine, heme *c*, quinohemoprotein

Many bacteria are able to use various amines as substrates for growth. These compounds are usually produced as intermediates in the synthesis or degradation of amino acids or other nitrogen-containing biomolecules and therefore are available in large amounts. Microbial amine degradation is initiated either by pyridoxal

Citation Schmitt G, Saft M, Arndt F, Kahnt J, Heider J. 2019. Two different quinohemoprotein amine dehydrogenases initiate anaerobic degradation of aromatic amines in *Aromatoleum aromaticum* EbN1. J Bacteriol 201:e00281-19. https://doi.org/10.1128/JB.00281-19.

Editor Michael Y. Galperin, NCBI, NLM, National Institutes of Health

Address correspondence to Johann Heider, heider@biologie.uni-marburg.de.

Received 18 April 2019
Accepted 23 May 2019
Accepted manuscript posted online 28 May 2019
Published 24 July 2019

phosphate-containing aminotransferases or by amine oxidases or dehydrogenases (1–3). In both cases, the amines are initially converted to aldehydes or ketones (from primary or secondary amines, respectively). Most of the known amine-oxidizing enzymes belong to the flavoenzymes and contain a flavin adenine dinucleotide (FAD) or flavin mononucleotide (FMN) cofactor in their active sites, but some are known as quinoenzymes, containing several types of quinoid cofactors (2, 4, 5). The first characterized quinoenzymes were methanol dehydrogenase (6, 7) and glucose oxidase, which contain the soluble cofactor pyrroloquinoline quinone (PQQ) in their active sites and oxidize alcohols or sugars rather than amines, but a growing number of additional amine-oxidizing quinoenzymes with covalently bound quinoid cofactors have been identified over the last 3 decades. The respective quinoid cofactors in these enzymes are derived from aromatic amino acids whose aromatic rings are posttranslationally hydroxylated and oxidized to *ortho*- or *para*-quinones and which are often additionally cross-linked with other amino acids of the same subunits (8, 9). Quinoid amine oxidases can be distributed in several classes, based on their sequences and the particular structures of their cofactors. The so-called copper amine oxidases contain a redox-active Cu ion in addition to their quinoid cofactors and represent two separate quinoenzyme classes containing either topaquinone (TPQ) or lysine tyrosylquinone (LTQ) as quinoid cofactors (8, 10, 11). Metal-independent quinoenzyme classes are represented by methylamine dehydrogenases, which contain a tryptophan tryptophylquinone (TTQ) cofactor, and by quinohemoprotein amine dehydrogenases, which contain a cysteine tryptophylquinone (CTQ) cofactor (12–15).

Two gene clusters coding for apparent periplasmic CTQ-containing quinohemoproteins were detected during genome sequencing in the anaerobic aromatic-degrading betaproteobacterium *Aromatoleum aromaticum* EbN1. However, this bacterium has not been known to degrade any biological amines, and no expression of the quinohemoprotein-encoding genes has been observed under any condition (16–18). We have established amines such as benzylamine (BAm), 2-phenylethylamine (2-PEA), and butylamine as new growth substrates for *A. aromaticum* under nitrate-reducing conditions and shown that either of the two isoenzymes encoded by the genome is specifically induced by the respective substrate, serving as the first enzyme of the respective degradation pathway. Degradation of the aromatic amines continues by further oxidation of the respective aldehydes to either phenylacetate (PA) or benzoate (Fig. 1), leading to their complete decomposition to CO_2 via the established pathways of anaerobic PA and benzoate metabolism (17, 19). To our knowledge, this is the first report of quinoid amine dehydrogenases being involved in a strictly anaerobic catabolic pathway.

RESULTS

Growth and enzyme activities of *A. aromaticum* EbN1 with aromatic amines. *A. aromaticum* EbN1 is known to grow with the aromatic amino acids Phe and Tyr as sole substrates (16), but growth on related amines has not been tested so far. We observed that this organism also grows very well on the primary aromatic amines benzylamine (BAm) and 2-phenylethylamine (2-PEA) under nitrate-reducing conditions, reaching an optimal growth rate of 0.11 h^{-1}, which is equal to that observed with Phe (20). In contrast, no growth was detected with one of the secondary amines (*R*)- and (*S*)-1-phenylethylamine as the substrate. BAm and 2-PEA are expected to be degraded via an initial conversion to the corresponding aldehydes and acids, respectively, which then enter the known degradation pathways of benzoate or phenylacetate (Fig. 1) (17, 19, 21). Conversion of the amines to aldehydes can principally be catalyzed either by aminotransferases or amine oxidases/dehydrogenases. Therefore, we tested cell extracts of *A. aromaticum* EbN1 grown with BAm or 2-PEA for both types of enzymes. No aminotransferase activities were observed; instead, either BAm- or 2-PEA-oxidizing activities were detected with dichloroindophenol (DCIP)-phenazine methosulphate (PMS) or ferricenium as an artificial electron acceptor. The highest activities were measured in cells grown with BAm or 2-PEA and reasonable activities were also present

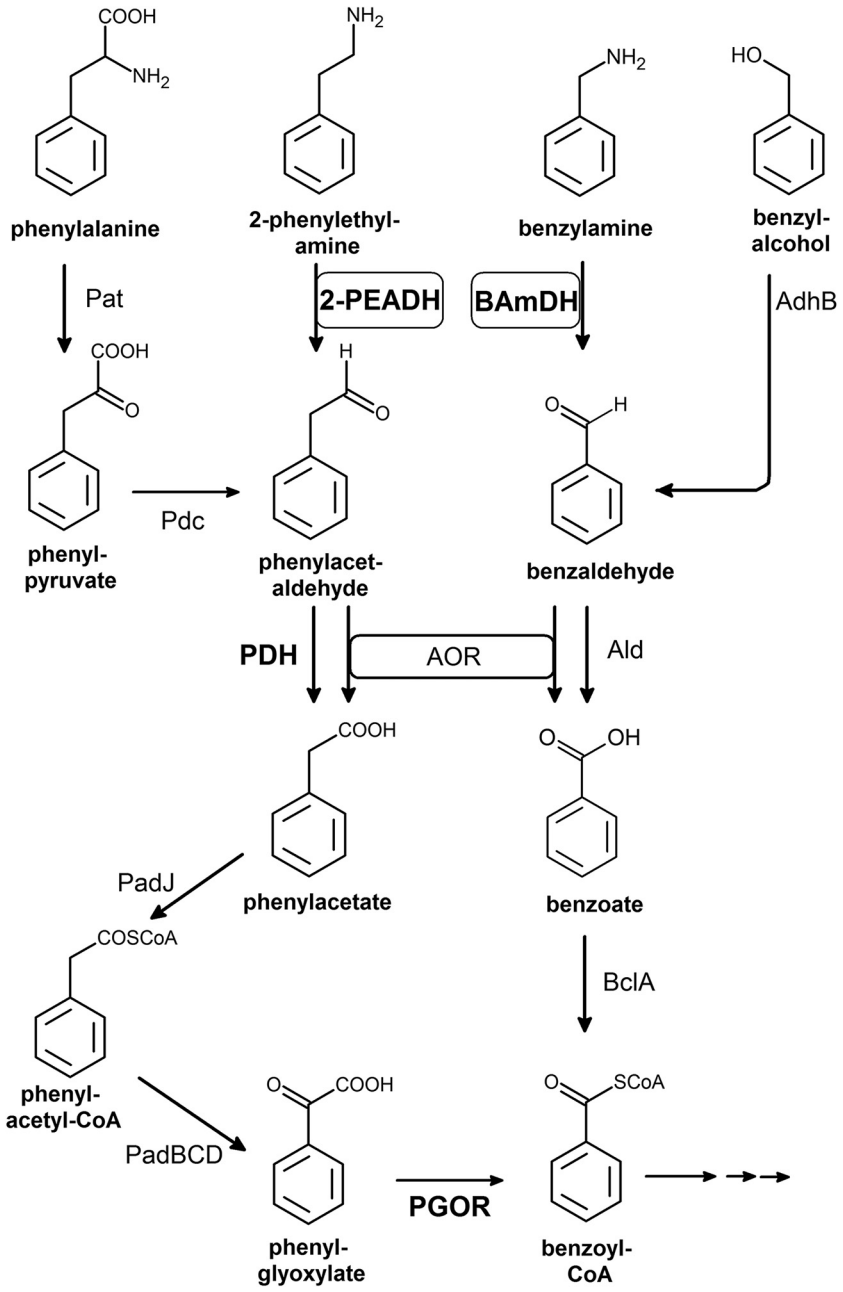

FIG 1 Anaerobic degradation of aromatic amines and other compounds in *A. aromaticum* EbN1, as relevant in this study. Enzymes (and associated genes): Pat, Phe aminotransferase (*ebA596*); Pdc, phenylpyruvate decarboxylase (*ebA6545*); AOR, aldehyde:ferredoxin oxidoreductase (*ebA5005*); PDH, phenylacetaldehyde dehydrogenase (*ebA4954*); PadJ, phenylacetate-CoA ligase (*ebA5402*); PadBCD, phenylacetyl-CoA:acceptor oxidoreductase (*ebA5393*, *ebA5395*, and *ebA5396*); PadEFGHI, phenylglyoxylate: acceptor oxidoreductase (PGOR) (*ebA5397*, *ebB191*, and *ebA5399* to *ebA5401*); AdhB, benzyl alcohol dehydrogenase (*ebA3118* or *ebA4623*); Ald, benzaldehyde dehydrogenase (*ebA5642*); BclA, benzoate-CoA ligase (*ebA5301*). Arrows leading away from benzoyl-CoA indicate the further degradation pathway via aromatic ring reduction and β-oxidation.

in cultures grown with Phe (Table 1), but only very low levels of activity ($<$10 nmol min^{-1} mg^{-1}) were found in extracts of cells grown with benzoate, PA, or ethylbenzene. Comparing the specific amine dehydrogenase activity levels toward BAm versus 2-PEA, extracts of BAm-grown cells showed a higher value for BAm ($>$100 nmol min^{-1} mg^{-1}) than for 2-PEA (45 nmol min^{-1} mg^{-1}) oxidation, while extracts of 2-PEA-grown cells showed a reversed pattern of activities (70 versus 40 nmol min^{-1} mg^{-1} with 2-PEA and

TABLE 1 Specific activities of diverse enzymes involved in anaerobic metabolism of the aromatic amines 2-PEA and BAm[b]

	Sp act (nmol min^{-1} mg^{-1}) for:							
					PDH		BAld DH	
Growth substrate (strain)	2-PEADH	BAmDH	AOR	PGOR	NAD	NADP	NAD	NADP
2-PEA (EbN1)	69	43	14*	250*	194*	414*	<1	155*
2-PEA (SR7_Δ*pdh*)	75	36	60*	49*	2*	0*	ND	ND
2-PEA (SR7_Δ*pdh*) (−W)**	38	18	0*	84	62	0	ND	ND
Phe (EbN1)	28	15	18[a]*	211[a]*	108[a]*	192[a]*	<1	161
PAld (EbN1)	ND	ND	8	281	29	55	1	59
BAm (EbN1)	43	108	16	9	57	1	98	215
Benzylalcohol (EbN1)	ND	ND	27[a]	15[a]	54[a]	70[a]	25	75
Benzaldehyde (EbN1)	ND	ND	20[a]	10[a]	21[a]	32[a]	47	66
Benzoate (EbN1)	7	3	11*	4*	3*	4*	5	179
Ethylbenzene (EbN1)	ND	ND	9	0.5	8	11	ND	ND

[a]Values from Schmitt et al. (20).

[b]The different strains (EbN1 or Δ*pdh* strain) and growth conditions (standard or without tungstate [−W]) used for cultures with 2-PEA are indicated. Standard deviations were <30% of the respective values. ND, not detectable; *, averaged from ≥3 independent cultures; **, culture transferred from strain SR7_Δ*pdh* (−W) adapted on Phe to 2-PEA.

BAm, respectively). The measured activities are sufficient to explain the recorded growth rates ($\mu = 0.11\ h^{-1}$ corresponds to a specific activity of 60 nmol min^{-1} mg^{-1}). The activities recorded in Phe- or benzoate-grown cells showed a pattern similar to that in 2-PEA-grown cells (Table 1). The clear difference in activities between the differently grown cultures indicated that there must be two separate isoenzymes, one present in BAm-grown cells and another one in the other studied cell batches. Moreover, the synthesis of both amine dehydrogenases appears to be specifically induced by the respective main growth substrates, i.e., BAm or 2-PEA.

Further degradation pathways of aromatic amines. In analogy to Phe or benzyl alcohol degradation in *A. aromaticum* EbN1 (20, 21), we expected that the aldehydes generated by the amine dehydrogenases are further oxidized by aldehyde dehydrogenases or a tungsten-containing aldehyde oxidoreductase (AOR). Cells grown with 2-PEA or Phe, but not with other substrates, indeed contained a highly specific phenylacetaldehyde dehydrogenase (PDH) using NAD or NADP as electron acceptors with a characteristic ratio of activities of 0.56, as described in reference 22 (Table 1). The presence of the enzymes of the subsequent PA catabolic pathway has been tested by measuring the key enzyme phenylglyoxylate-oxidoreductase (PGOR), which was active in all cells grown with substrates entering the PA catabolic pathway (Table 1) but was virtually absent from cells grown with BAm, benzyl alcohol, benzoate, or ethylbenzene. In contrast, cells grown with BAm contained an apparently induced NAD-dependent benzaldehyde dehydrogenase (BAld-DH), which was also recorded in benzyl alcohol (BAlc)- or BAld-grown *A. aromaticum* EbN1 cells (Table 1) and probably represents the same enzyme as that present in BAm-grown cells.

Additionally, low activities of the recently characterized tungsten-containing AOR (23) were observed in all cells grown with BAm, 2-PEA, Phe, benzyl alcohol, or benzaldehyde, while it was almost absent from control cells grown with benzoate, PA, or ethylbenzene (Table 1). This corroborates the proposed function of AOR for aldehyde detoxification, because all inducing substrates are degraded via aldehyde intermediates (24).

We also checked the degradative activities of a deletion mutant of *A. aromaticum* lacking the gene for PDH (strain SR7_Δ*pdh*), which compensates for this enzyme with a markedly increased AOR activity (20). The mutant also grew with 2-PEA reaching slightly lower growth rates than the wild type and exhibited similar specific activities of 2-PEA dehydrogenase (Table 1). In the absence of tungstate, strain SR7_Δ*pdh* reached optical density (OD) values of only 0.2 to 0.3 with 2-PEA and could not be further maintained with this substrate. However, a derivative of strain SR7_Δ*pdh*, which has adapted to growth on Phe in the absence of tungstate by using a mutant version of the *aldB* gene product as an alternative NAD-dependent phenylacetaldehyde (PAld) dehy-

TABLE 2 Enrichment of BAmDH activity from *A. aromaticum* EbN1 grown on BAm and of 2-PEADH activity from strain SR7_Δ*pdh* grown with 2-PEA[a]

Step and enrichment type	Total protein (mg)	Total act (U)	Yield (%)	Sp act (nmol min^{-1} mg^{-1})		Enrichment (fold)
				BAmDH	2-PEADH	
BAmDH, *A. aromaticum* EbN1						
Soluble cell extract	257	27.5	100	103		1
DEAE-Sepharose	18.3	18.8	68.3	1,286		12.4
Hydroxyapatite (CHT-I)	4.3	14.3	52	4,286		41.4
2-PEA, strain SR7_Δ*pdh*						
Soluble cell extract	976	21.7	100		22.2	1
DEAE-Sepharose	103	11.9	50.2		119	5.3
Hydroxyapatite (CHT-I)	5.6	5.04	23.2		1,121	50.4

[a]Data shown are for enrichment of BAmDH activity from 7.2 g cell wet mass of *A. aromaticum* EbN1 grown on BAm and enrichment of 2-PEADH activity from 20 g cell wet mass of strain SR7_Δ*pdh* grown with 2-PEA.

drogenase (20), also grows with 2-PEA (Table 1). The presence of PAld in the supernatants of these cultures was verified by an enzymatic assay using purified PDH, indicating PAld accumulation up to 160 μM in the stalled cultures of strain SR7_Δ*pdh* in the absence of tungstate, while only 5 to 6 μM PAld was detected in the growing cultures of the wild-type strain EbN1 or strain SR7_Δ*pdh* in the presence of tungstate.

In the wild-type strain, growth capabilities similar to those observed for the aromatic amines were expected if the corresponding alcohols, BAlc or 2-phenylethanol (2-PE), were offered as sole substrates. Growth of *A. aromaticum* EbN1 with BAlc has been recognized and studied before (17, 20), and the enzyme activities obtained from cultures grown with benzyl alcohol or benzaldehyde (Table 1) indicate that benzylamine shares the same downstream metabolic pathway. However, 2-PE surprisingly did not support growth under nitrate-reducing conditions, even at lowered concentrations to avoid potential toxic effects or after prolonged incubation times of up to 6 weeks. Therefore, *A. aromaticum* EbN1 apparently does not produce a 2-PE oxidizing alcohol dehydrogenase under these conditions.

Identification and properties of amine dehydrogenases I and II. The two amine dehydrogenase isoenzymes were purified from either BAm- or 2-PEA-grown cells via the same protocol, using ion-exchange chromatography on DEAE-Sepharose in a first step and chromatography on hydroxyapatite (CHT-I) in a second step. The two enzymes showed marked differences in their binding properties to the column materials, as described in Materials and Methods. The amine dehydrogenase from BAm-grown cells was 41-fold enriched, leading to a virtually pure enzyme (here called BAmDH), whereas the amine dehydrogenase from 2-PEA-grown cells (here called 2-PEADH) was 50-fold enriched but was only obtained at ca. 60% purity, as judged from SDS-PAGE analysis (Table 2 and Fig. 2A and B). Both preparations showed major bands at 60 and 40 kDa after SDS-PAGE, which were cut out and verified by matrix-assisted laser desorption ionization–time of flight (MALDI-TOF) analysis of tryptic fragments as the large (α) and medium (β) subunits of two previously annotated quinohemoprotein amine dehydrogenases from the genome of *A. aromaticum* EbN1 (16). The expected small subunits (γ) of 11 kDa were not visible on SDS gels (GenBank accession numbers CAI07354 and CAI09067, with the sequence of the latter manually extended assuming an alternative start codon). A 16-kDa protein in the enriched 2-PEADH preparation was considered a potential candidate for the γ-subunit (Fig. 2B) but was identified as a thioesterase (ebB192 gene product) by MALDI-TOF analysis, suggesting that it represents a contaminating protein. However, MALDI-TOF analysis of the native preparation of 2-PEADH revealed the presence of N- and C-terminal peptides of the respective γ-subunit (residues A11-K25, W85-K105, D90-K105, and D95-K105) and confirmed the presence of this subunit. The observed N-terminal peptide is contained in the predicted signal sequence of the γ-subunit, suggesting only partial proteolytic processing in the mature enzyme. The γ-subunits of quinohemoproteins of this family are expected to be

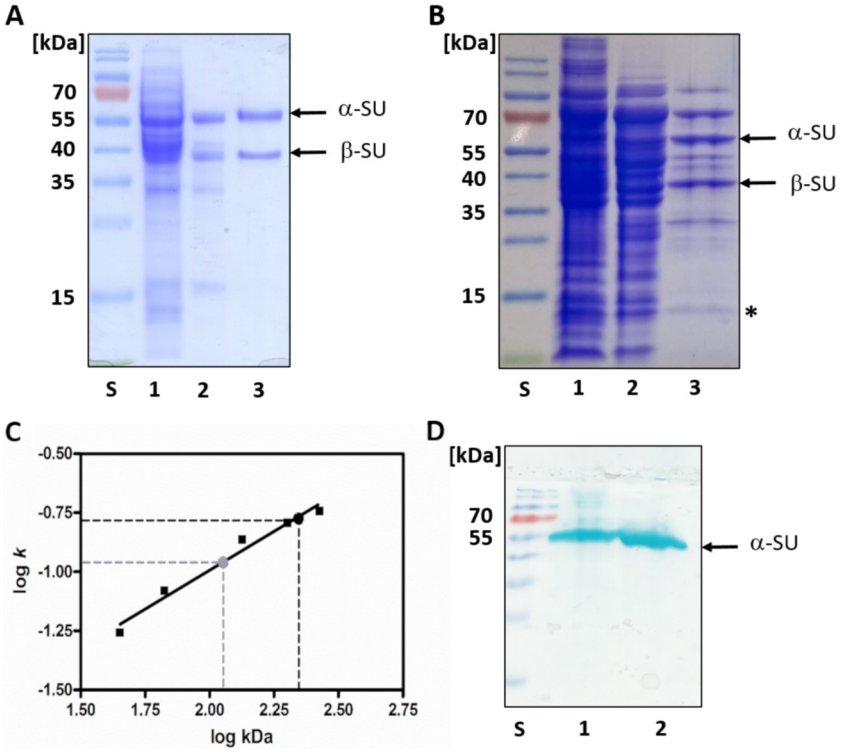

FIG 2 Molecular properties of BAmDH and 2-PEADH. (A and B) SDS-PAGE analysis of the respective fractions during purification of BAmDH (A) and 2-PEADH (B). Lanes: S, molecular mass standard; 1, cell extract; 2, DEAE-Sepharose pool; 3, hydroxyapatite pool. The identified subunits are indicated; the asterisk indicates a contaminating protein unrelated to 2-PEADH. (C) Ferguson plot analysis of native enzymes. The slopes from plotting the relative migration rates versus concentrations of native polyacrylamide gels (*k*) were plotted against standard protein masses in double-logarithmic scale, yielding masses of 219 kDa for 1-PEDH and 114 kDa for BAmDH. (D) Heme staining of 2-PEADH (lane 1) and BAmDH (lane 2). Lane S, molecular mass standard.

heavily modified by the products of several further genes in the respective operons, which insert four thioether cross-links involving the four cysteines present in the sequence (C36, C56, C65, and C69) and generate a CTQ cofactor (25, 26). The internal thioether cross-links appear to impede detection via SDS-PAGE, because the peptide chains cannot be unfolded by SDS and prevent the production of small tryptic fragments from the central part of the subunits. Accordingly, all detected peptides from the γ-subunits are derived from regions outside the cross-linked core region. The amino acid sequence identities between the two isoenzymes of *A. aromaticum* EbN1 are 43% for the α-subunits, 45% for the β-subunits, and 58% for the γ-subunits. Very similar quinohemoprotein amine dehydrogenases have recently been characterized, and crystal structures are known from *Paracoccus denitrificans* (27) and *Pseudomonas putida* (28) (identities of 34% to 67%) (Table 3). Because of the high degree of sequence conservation of the γ-subunits and full conservation of all modified amino acids (29), the same modification patterns and the same mechanisms of secretion to the periplasmic space are expected for 2-PEADH and BAmDH.

Molecular properties. The native molecular masses of the two isoenzymes were determined by Ferguson plot analysis of their migration in native polyacrylamide gels, resulting in values of 219 kDa for 2-PEADH and 114 kDa for BAmDH, respectively (Fig. 2C). The value for BAmDH corresponds well to the reported masses and structures of the previously characterized orthologues from *P. putida* and *P. denitrificans* (12, 27, 28), indicating a heterotrimeric $\alpha\beta\gamma$ composition, whereas the doubled mass of 2-PEADH indicates a heterohexameric $\alpha_2\beta_2\gamma_2$ composition. Signal peptides ranging between 19 and 42 amino acids are predicted at the N termini of all three subunits of both isoenzymes (Table 3), as reported for the enzymes of *P. putida* and *P. denitrificans* (27,

TABLE 3 Properties of 2-PEADH, BAmDH, and the amine dehydrogenases of *P. putida* and *P. denitrificans*

Parameter	Value(s) for[c]:			
	2-PEADH	BAmDH	*P. putida*	*P. denitrificans*
Predicted size (aa/Da)	921/101,543	921/102,122	921/102,974	908/99,958
Predicted pI	6.23	5.51	6.12	4.76
Signal peptides (aa $\alpha/\beta/\gamma$)	32/29/31	42/19/29	48/30/29	23/21/28
BAmDH (% $\alpha/\beta/\gamma$)	43/45/65			
P. putida (% $\alpha/\beta/\gamma$)[a]	43/34/67	44/34/64		
P. dentrificans (% $\alpha/\beta/\gamma$)[b]	43/34/69	42/36/64	42/33/65	

[a]*P. putida* α-subunit accession number BAB72008.
[b]*P. denitrificans* α-subunit accession number WP_011747998.
[c]The indicated masses, pI values, and sequence identities correspond to the parameters predicted for an $\alpha\beta\gamma$ protomer of the respective enzymes lacking the predicted or identified signal peptides of all three subunits and containing two heme *c* cofactors and the covalent modifications of the γ-subunits. The signal peptides of 2-PEADH and BAmDH were predicted from an alignment with the characterized enzymes. aa, summed number of amino acids of all three subunits; aa $\alpha/\beta/\gamma$, predicted signal peptide lengths; % $\alpha/\beta/\gamma$, calculated pairwise identities of the three subunits.

28, 30). The large differences in signal peptide lengths seem unusual but are also observed for other members of this enzyme family (Table 3), indicating still-unknown details in exporting these enzymes to the periplasm. We have predicted the most plausible proteolytic processing sites of all subunits from a multiple alignment including the characterized enzymes from *P. putida* and *P. denitrificans* and base our further calculations on these data (Table 3). Sequence comparison of the three subunits between the different enzymes suggested that the distances of the two isoenzymes of *A. aromaticum* EbN1 and the enzymes of *P. putida* and *P. denitrificans* are about equal, with 42 to 43% identity between the α-subunits, 33 to 35% between the β-subunits, and 64 to 69% between the γ-subunits (Table 3). The higher identity values of the α- and γ-subunits may reflect the necessity of posttranslational processing.

The heme *c* content of the isoenzymes was confirmed by heme staining after separating the subunits via SDS-PAGE (Fig. 2D). As expected, activity was detected exclusively in the 60-kDa band corresponding to the heme *c*-binding α-subunit (Fig. 2D). From sequence alignments, we predict two highly conserved heme *c* binding sites ($C_{44}AAC_{47}$ and $C_{133}ARC_{136}$ in 2-PEADH and $C_{58}GAC_{61}$ and $C_{145}ARC_{148}$ in BAmDH) and identical axial heme coordination, as shown for the enzymes from *P. denitrificans* and *P. putida* (28), namely, His and Met as axial ligands for the first and two His for the second heme (H_{48}/M_{76} and $H_{134/159}$ for 2-PEADH and H_{59}/M_{88} and $H_{149/181}$ for BAmDH). The amount of heme *c* was estimated from the recorded absorption values at 550 nm of the completely reduced proteins ($\varepsilon = 24.3\ mM^{-1}\ cm^{-1}$), yielding values of 1.77 heme/$\alpha\beta\gamma$ protomer for BAmDH and 1.17 heme/$\alpha\beta\gamma$ protomer for 2-PEADH. Regarding the low purity of the latter preparation (estimated at 60%) and the apparent absence of any other heme *c*-containing protein, the actual heme *c* content of 2-PEADH may be corrected to 1.95 heme/$\alpha\beta\gamma$ protomer.

Spectroscopic properties. The UV-visible (UV-Vis) spectra of BAmDH and 2-PEADH were similar to those reported for other quinohemoprotein amine dehydrogenases (12, 13). The spectra are dominated by the absorption of the heme *c* cofactors, which show the typical Soret band at 407 or 410 nm and broad absorption features around 523 to 525 nm for oxidized 2-PEADH and BAmDH, respectively (Fig. 3). Upon reduction, the Soret bands are shifted and the α-bands appear as doublets, resulting in absorption maxima at 416, 548, and 552 nm for 2-PEADH and at 419, 549, and 555 nm for BAmDH (Fig. 3). Splitting of the α-band appears in both isoenzymes and is more pronounced in BAmDH than in 2-PEADH, suggesting that the two heme *c* cofactors of the α-subunits have slightly different spectroscopic properties. A similar effect also occurs to a lesser degree in the published spectra of other quinohemoproteins (31) but has not been reported before. Similar cases of split α-bands are known in the spectra of other di-heme *c* enzymes (32). In addition to the heme-related absorption bands, both

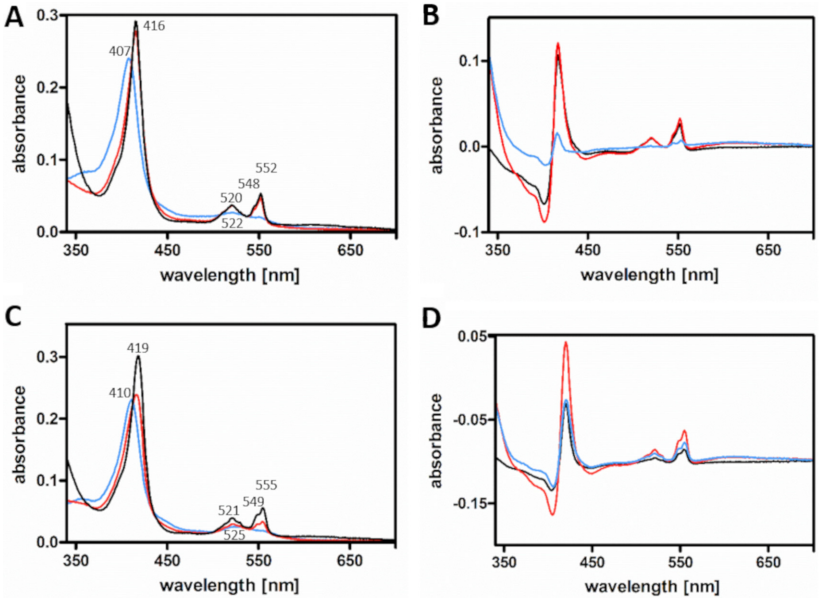

FIG 3 (A and C) UV-Vis spectra of 2-PEADH (A) and BAmDH (C) as isolated (blue), after reduction by substrate (red), and after chemical reduction by dithionite (black). (B and D) Difference spectra of 2-PEADH (B) and BAmDH (D) indicate the spectral changes upon reduction by substrate (black) or reduction by dithionite (red). The difference between dithionite-reduced and substrate-reduced forms is shown in blue.

isoenzymes exhibit absorption shoulders around 380 nm in the oxidized state, which decrease upon reduction and may be related to the quinoid CTQ cofactor, as proposed previously (12, 13, 31).

Only 2-PEADH was reduced (almost) completely by adding stoichiometric amounts of the substrate 2-PEA, whereas BAmDH was reduced only to 50% with BAm as the substrate, judging from the difference spectra with the fully reduced enzymes using dithionite as the reductant. Moreover, the heme *c* absorption patterns suggest the simultaneous reduction of both heme *c* groups (Fig. 3).

Catalytic properties. BAmDH and 2-PEADH were routinely assayed with a mixture of DCIP and PMS as artificial electron acceptors, as established for other quinohemoproteins (13, 33), but showed more than 10-fold-reduced activities with DCIP alone (Table 4). Therefore, we assume that PMS acts as the actual electron acceptor for the enzymes and reduces DCIP chemically. Both isoenzymes also showed good activities with ferricenium hexafluorophosphate or potassium ferricyanide as electron acceptors but with marked differences between the isoenzymes. 2-PEADH used both compounds equally well, whereas BAmDH showed a >10-fold higher rate with ferricenium than with ferricyanide (and 5-fold faster than that with DCIP-PMS). To test for the involvement of cytochrome *c* as a physiological periplasmic electron acceptor, as described for *P. denitrificans* (34), we assayed the activity of both isoenzymes with horse heart cytochrome *c* and found good activities, which amounted to 30% and 120% of the rates

TABLE 4 Electron acceptor preferences of 2-PEADH and BAmDH

Compound	Acceptor preference (%) for[a]:	
	2-PEADH	BAmDH
DCIP	6.2 (±0.4)	8.0 (±1.8)
DCIP-PMS	100 (±16)	100 (±13)
Ferricenium	157 (±12)	505 (±107)
Ferricyanide	138 (±9.4)	45 (±1.6)
Cytochrome *c* (horse heart)	32 (±1.4)	120 (±12)

[a]Electron acceptor preferences of 2-PEADH and BAmDH were measured with either 2-PEA (2-PEADH, 100% = 0.54 U mg^{-1}) or BAm (BAmDH, 100% = 4.4 U mg^{-1}) as the substrate. Standard deviations are indicated.

TABLE 5 Substrate spectra of 2-PEADH and BAmDH, using DCIP-PMS as electron acceptors[a]

	Sp act (nmol min^{-1} mg^{-1}) for:	
Substrate	**2-PEADH**	**BAmDH**
2-PEA	566	325
(*R*)-1-PEA	0	<25
(*S*)-1-PEA	0	<25
Benzylamine	264	4,680
Tyramine	469	243
p-Aminobenzoate	<25	0
Butylamine	258	0
GABA	<25	0
6-*N*-Capronic acid	<25	74.0

[a]Standard deviations were lower than 28%. Note that activities below 25 nmol min^{-1} mg^{-1} were detectable but yielded error deviations too high to indicate reliable values.

measured with DCIP-PMS for 2-PEADH and BAmDH, respectively. No activity of either isoenzyme was observed with oxygen as the electron acceptor by measuring H_2O_2 formation in an aerobic coupled assay with horseradish peroxidase and 2,2′-*azino*-bis(3-ethylbenzothiazoline-6-sulfonic acid (ABTS) or by measuring product formation in a coupled assay with PDH and NAD (see Materials and Methods).

Regarding the specific induction of the two isoenzymes in cells grown with BAm or 2-PEA, the substrate specificities of the two isoenzymes were of great interest. The isoenzymes indeed exhibited different activities with different substrates, especially BAm and 2-PEA (Table 5). 2-PEADH showed the highest activities with 2-PEA and tyramine and was still highly active with BAm and the aliphatic butylamine. It showed only marginal activities with γ-aminobutyrate or 6-aminocaproate and was inactive with (*R*)- or (*S*)-1-phenylethanol. In contrast, BAmDH was most active with BAm, exhibiting a 7-fold higher specific activity than the highest recorded activity of 2-PEADH, whereas the rate with 2-PEA was about half of that observed for 2-PEADH. With tyramine, only a short burst of activity was detected, followed by apparent self-inactivation within 2 min. BAmDH showed low activity with 6-aminocaproate and marginal activity with (*R*)- or (*S*)-1-phenylethanol (Table 5). In contrast to 2-PEADH, BAmDH did not turn over 1-butylamine but was strongly inhibited by this compound (see below). Therefore, the active sites involved in amine oxidation appear to be considerably different between the two isoenzymes. Based on these recorded activities, we tested whether *A. aromaticum* EbN1 grows with some of these substrates under nitrate-reducing conditions and recorded growth with 1-butylamine ($\mu = 0.06\ h^{-1}$) but not with either (*R*)- or (*S*)-1-phenylethylamine.

To understand further the catalytic properties of the isoenzymes, we determined the apparent kinetic parameters for some substrates. 2-PEADH exhibited a 3-fold higher apparent V_{max} but only a slightly better apparent K_m value for 2-PEA than for BAm (Table 6). The values for the aliphatic substrate 1-butylamine indicated substrate-inhibition kinetics, yielding an apparent V_{max} of 350 nmol min^{-1} mg^{-1}, an apparent K_m of 2.11 mM, and a substrate inhibition constant, K_i, of 46.5 mM (Table 6). Because of the effects of substrate inhibition, the theoretical V_{max} was not accessible and the maximal observed activity was 250 nmol min^{-1} mg^{-1} (Fig. 4D). Conversely, BAmDH showed a 16-fold higher apparent V_{max} for BAm than for 2-PEA, while the apparent K_m value for BAm was 5-fold higher than that for 2-PEA (Table 6). The calculated catalytic efficiencies indicate clearly that 2-PEA is the preferred substrate of 2-PEADH (4-fold higher k_{cat}/K_m value than that for BAm), and BAm is preferred by BAmDH (3-fold higher k_{cat}/K_m value than that for 2-PEA). Both enzymes also appear to prefer aromatic over aliphatic aldehydes, as inferred from the rather low catalytic efficiency of 2-PEADH and inhibition of BAmDH with 1-butylamine (Table 6 and Fig. 4).

Inhibition. Typical quinohemoprotein inhibitors like the carbonyl reagents hydroxylamine and phenylhydrazine (13, 35) inhibited both enzymes from *A. aromaticum* EbN1 irreversibly. Addition of 5 μM phenylhydrazine to the assay resulted in about 80%

TABLE 6 Apparent kinetic parameters of the oxidation of selected amines by quinohemoprotein amine dehydrogenase 2-PEADH or BAmDH coupled to DCIP-PMS

Enzyme and substrate	V_{max} (nmol min^{-1} mg^{-1})	K_m (μM)	K_i (μM)	k_{cat} (s^{-1})[a]	k_{cat}/K_m (mM^{-1} s^{-1})	R^{2b}
2-PEADH						
2-PEA	631	142		1.15	8.11	0.957
Benzylamine	202	197		0.370	1.88	0.934
Butylamine	350	2.10×10^3	4.65×10^4	0.640	0.300	0.975
BAmDH						
2-PEA	260	72.6		0.470	6.50	0.946
Benzylamine	4.17×10^3	346		7.58	21.9	0.961
Butylamine	ND[c]					

[a]Values for k_{cat} are given per $\alpha\beta\gamma$ protomer.
[b]The R^2 values indicate the respective fitting qualities.
[c]ND, no activity detected.

inhibition of 2-PEADH and 90% inhibition of BAmDH activity in a concentration-dependent manner (Fig. 4A), and the inhibitory effects on both enzymes were even more pronounced after 2 min of preincubation before starting the assays (data not shown). Hydroxylamine inhibited BAmDH activity completely at 1 μM but showed much lower effects on 2-PEADH activity, which retained 81% of its activity in the presence of 1 μM hydroxylamine and still showed 5% activity in the presence of 100 μM hydroxylamine.

We also identified propionaldehyde as a product-like inhibitor for BAm oxidation by BAmDH, leading to 85% inhibition at 2 μM (Fig. 4B), whereas it did not affect 2-PEA oxidation by BAmDH (84% activity retained) or the oxidation of either aromatic amine by 2-PEADH (>95% activity retained) under the same conditions. Finally, the kinetic analysis of 1-butylamine oxidation by 2-PEADH revealed substrate inhibition at higher concentrations (Fig. 4D). The values of the apparent catalytic parameters were obtained

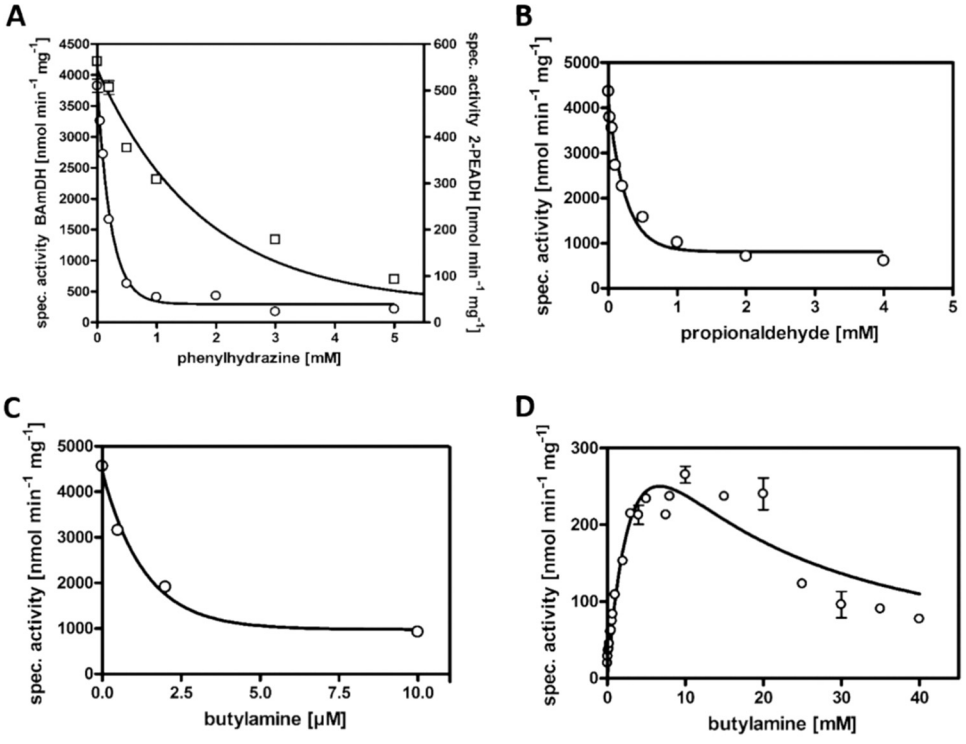

FIG 4 Inhibition of 2-PEADH and BAmDH. (A) Inhibition of BAmDH (□, left axis) and 2-PEADH (○, right axis) by phenylhydrazine using 2-PEA and BAm as substrates. (B and C) Inhibition of BAm oxidation via BAmDH by propionaldehyde (B) and butylamine (C). (D) Substrate inhibition of 2-PEADH by butylamine.

by nonlinear curve fitting and are indicated in Table 6. Because BAmDH did not turn over butylamine as a substrate, we assessed it as a potential inhibitor of BAm oxidation and observed a strong inhibitory effect, resulting in 75% inhibition in the presence of 10 μM butylamine (Fig. 4C).

DISCUSSION

Although the aerobic degradation of aromatic amines has been described for a number of bacteria (36–39), no experimental evidence has been available for their conversion under anoxic conditions. Genome analysis of *A. aromaticum* EbN1 and *Azoarcus* sp. strain CIB has previously revealed the presence of gene clusters coding for quinohemoprotein-type amine dehydrogenases (21, 40). In this report, we demonstrate the utilization of 2-PEA and BAm by *A. aromaticum* EbN1 with high growth rates under anoxic, nitrate-reducing conditions and identify and characterize two different periplasmic quinohemoprotein amine dehydrogenases previously predicted from genome analysis as the respective initial enzymes. 2-PEA, the amine derived from the amino acid Phe, is channeled into the Phe degradation pathway after it is oxidized to PAld by 2-PEADH. This is confirmed by similar adaptive complementations of the degradation pathways of Phe or 2-PEA in a knockout mutant lacking PDH (strain SR7_Δ*pdh*). PDH activity was replaced by increased AOR activity in the presence or by another induced NAD-specific aldehyde dehydrogenase (AldB) in the absence of tungstate (20), although the observed growth rates of the adapted strains were lower than those of the wild-type cells, and the AldB-overproducing mutant did not arise spontaneously in 2-PEA-degrading cultures, as observed with Phe (20). This may be explained by a higher rate of PAld production from 2-PEA than from Phe, as indicated by significantly increased PDH activities in wild-type cells grown with 2-PEA compared to that with Phe and high PAld accumulation in failed cultures of strain SR7_Δ*pdh* with 2-PEA in the absence of tungstate.

During growth with BAm, the cells shift completely to the other isoenzyme encoded by the genome, BAmDH, which exhibits a higher turnover rate with BAm than with 2-PEA and differs from 2-PEADH in its substrate recognition and inhibition properties. Both enzymes from *A. aromaticum* EbN1 showed the highest recorded activities with the aromatic amines Bam and 2-PEA (and tyramine for 2-PEADH), and the observed turnover rates of these substrates are in the same range as those reported for the related quinohemoproteins from *P. putida* and *P. denitrificans* (31, 35). In contrast, the aliphatic 1-butylamine turned out to be a poor substrate for 2-PEADH and as an inhibitor for BAmDH, whereas it is oxidized 2-fold faster than the aromatic amines by the enzymes of *P. putida* and *P. denitrificans* (13, 33, 35). Together with the observed specific induction of the respective enzymes, this indicates that the physiological function of 2-PEADH and BAmDH in *A. aromaticum* EbN1 is indeed the oxidation of aromatic amines.

Genes for enzymes of the quinohemoprotein family are present in the genomes of many proteobacterial species. Most of these are affiliated with the *Alpha-*, *Beta-*, and *Gammaproteobacteria*, but an orthologue is also present in the sulfate-reducing deltaproteobacterium *Desulfobacula toluolica* and the epsilonproteobacterium *Arcobacter butzleri* (Fig. 5). In addition, some strains affiliated with the *Firmicutes* and the *Acidobacteria* contain similar orthologues. A phylogenetic tree constructed from the concatenated sequences of the three conserved subunits indicates that 2-PEADH, BAmDH, and the previously characterized quinohemoproteins from *P. putida* and *P. denitrificans* belong to different subbranches among most proteobacterial species (Fig. 5A). BAmDH is most similar to the (single-copy) orthologues from related *Aromatoleum* or *Azoarcus* strains, whereas 2-PEADH forms a common subbranch with orthologues from *Thauera* strains but also from a *Pseudomonas* sp. Other subbranches consist of sequences from mixed strains of *Alpha-*, *Beta-*, and *Gammaproteobacteria* (Fig. 5A). In many cases, the genes are only present in a few strains affiliated with certain genera or species, suggesting a large contribution of lateral gene transfer in the spreading of the genes. The sequences from *D. toluolica*, the *Firmicutes*, and the *Acidobacteria* (together with

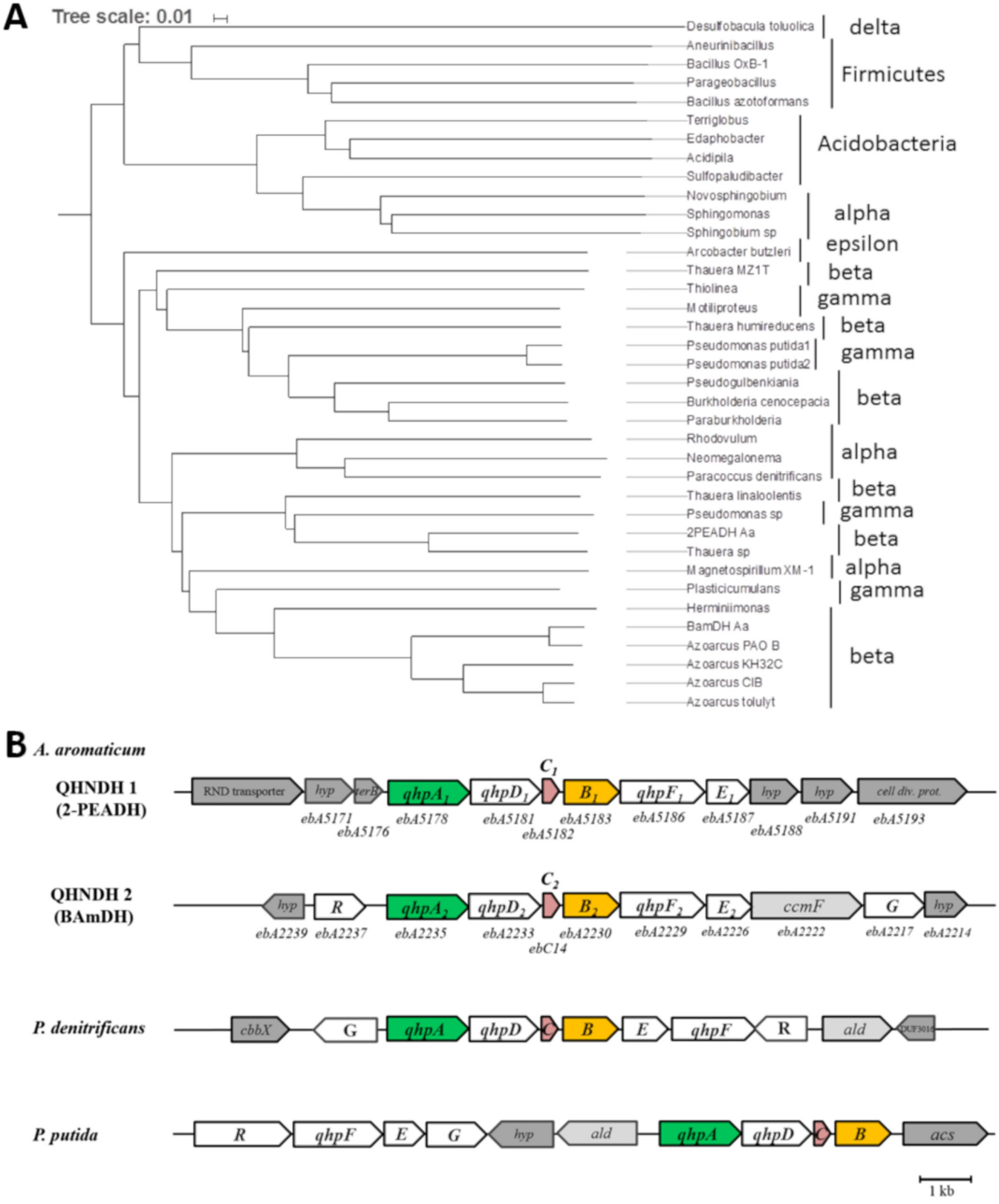

FIG 5 Phylogenetic analysis and operon structure of amine dehydrogenases. (A) The concatenated amino acid sequences of the subunits α, β, and γ from selected organisms of different phyla were aligned and used to construct a phylogenetic tree. The root was tentatively set between the majority of the proteobacterial strains and those from the *Firmicutes* and *Acidobacteria*. GenBank accession numbers of the respective α-subunits, from top to bottom: WP_014956167, ERI07627, BAQ11975, ANZ31294, KEF39273, WP_083344387, WP_130421394, WP_117303431, WP_105502221, WP_133721779, WP_039997591, WP_004210956, WP_004510534, ACR01581, WP_020393927, WP_076721259, AMO38522, KWW11764, BAB72008, BAK77010, AIO35069, WP_134759682,

(Continued on next page)

some *Alphaproteobacteria* affiliated with the *Sphingomonadales*) show only quite low similarities to those of the characterized enzymes (Fig. 5A). Although the lowest identity levels between the concatenated sequences shown were below 25%, the identification of all these enzymes as related quinohemoproteins is clearly evident from the universal conservation of all important sequence motifs, such as the two heme *c* binding sites, including the axial ligands in the α-subunits, as well as all four Cys residues, the Trp contained in the CTQ cofactor, and the other three respective binding partners of the thioether bridges in the γ-subunits (25, 26). Interestingly, the conserved Trp residue involved in forming the CTQ cofactor is preceded by another Trp in almost all sequences, which is replaced by Phe or Tyr in all sequences from *Acidobacteria* and *Sphingomonadales*, forming a distant common subbranch in the phylogenetic tree (Fig. 5A). In addition, all strains carrying these genes show a similar genomic context. In particular, the genes for the three subunits (*qhpABC* for the α-, β-, and γ-subunits, respectively) are always accompanied by a *qhpD* gene coding for an *S*-adenosylmethionine (SAM)-radical enzyme (Fig. 5B), which has been implicated in forming the four thioether bonds in the γ-subunit (29), and most of the gene clusters contain additional genes coding for further maturation enzymes (Fig. 5B). The presence of two different quinohemoprotein operons in parallel, as in *A. aromaticum* EbN1, appears to be rather rare in nature, because only a few bacteria have been found to carry two copies of the genes (15). While many of the identified bacterial quinohemoprotein gene clusters are also accompanied by genes encoding enzymes potentially involved in the further degradation pathway, such as aldehyde dehydrogenases, Mo-containing aldehyde hydroxylases, or acyl coenzyme A (acyl-CoA) synthetases (Fig. 5B, *P. putida* and *P. denitrificans*), the two clusters coding for 2-PEADH and BAmDH in *A. aromaticum* EbN1 show no such connection to the genes coding for the further enzymes of the pathway. However, they are flanked by several additional genes, which are usually found as part of quinohemoprotein gene clusters and code for maturation enzymes (Fig. 5B).

One of the gene clusters of *A. aromaticum* EbN1 contains the genes for the subunits of 2-PEADH, which form an apparent operon with genes for the maturation factors QhpD1, QhpE1, and QhpF1 (Fig. 5B, genes *ebA5478* to *ebA5187*). The other gene cluster (genes *ebA2235* to *ebA2217*) consists of the genes for the subunits of BAmDH in an apparent operon with *qhpD2*, *qhpE2*, and *qhpF2*, coding for separate copies of maturation factors, a *ccmF* paralogue, coding for a putative heme *c* insertion factor, and *qhpG*, coding for a quinohemoprotein maturation factor missing from the gene cluster for 2-PEADH. In addition, the gene cluster for BAmDH is flanked by a gene for a putative transcription regulator (*qhpR*) that may be involved in the apparent induction during growth with BAm (Fig. 5B). From studies on *P. denitrificans*, QhpD has been shown to catalyze the successive formation of the four thioether bonds in the γ-subunit, resulting in one Cys-Trp, one Cys-Glu, and two Cys-Asp cross-links (26). Further studies on the membrane-bound transport protein QhpF have shown that it is involved in the export of the modified γ-subunit to the periplasm, which is apparently accompanied by the cleavage of its nonstandard signal peptide by the serine protease QhpE (15, 29). Finally, a role of QhpG has been implied in converting the cross-linked Cys-Trp thioether to the quinoid CTQ cofactor in an O_2-dependent process (15). In the case of the two enzymes of *A. aromaticum* EbN1, it seems obvious that copies of QhpD, QhpE, and QhpF are coexpressed with the respective isoenzymes and have the same functions in thioether formation and periplasmic export of the γ-subunit as those characterized in *P. denitrificans* (QhpDEF identities of 30% to 58%). However, the mechanism of generating the quinoid modification of CTQ appears quite unclear, although there is at least one copy

FIG 5 Legend (Continued)
WP_081535881, WP_018634151, QAR25204, WP_004348003, WP_103319347, CAI07356, PZU51007, CUW39600, WP_132538231, WP_051566717, CAI09065, WP_082308102, WP_015436627, WP_050416583, and WP_076601108. (B) Operon structures of the genes coding for 2-PEADH and BAmDH of *A. aromaticum* EbN1 as well as the quinohemoproteins of *P. denitrificans* and *P. putida*. Gene names: *qhpABC*, amine dehydrogenase structural genes; *qhpD*, SAM-radical enzyme; *qhpE*, subtilisin-like protease; *qhpF*, translocase; *qhpG*, FAD-dependent monooxygenase; *ccmF*, heme *c* insertion factor; *acs*, CoA ligase; *ald*, aldehyde dehydrogenase; *hyp*, gene for hypothetical protein; *R*, gene for potential regulator.

of a QhpG-like protein (35% identity) encoded by the gene cluster for BAmDH (Fig. 5B). Because the two enzymes of *A. aromaticum* EbN1 are produced in active forms under strictly anoxic growth conditions, it is apparent that the quinoid cofactor does not require molecular oxygen for its formation. It remains to be tested whether QhpG takes part in an oxygen-independent hydroxylation reaction or whether additional maturation factors are required. The gene cluster for BAmDH also contains an additional gene for a membrane-bound cytochrome *c* maturation enzyme (CcmF), which is likely involved in supplying heme *c* to the α-subunit in the periplasmic space (41). The other copy of a *ccmF* gene is located in the *ccm* gene cluster predicted to code for enzymes involved in cytochrome *c* maturation (21). It is an open question whether the *ccmF* and *qhpG* gene products are required as maturation factors for both quinohemoproteins or whether their functions can be taken over by other proteins of the cells. The observed operon organization suggests that expression of these two genes particularly boosts the production of active BAmDH under inducing growth conditions when the activity of the normal biosynthetic machinery becomes limiting.

MATERIALS AND METHODS

Growth of bacteria. *Aromatoleum aromaticum* strain EbN1 and the SR7 and SR7_Δ*pdh* derived mutants (20, 42) were grown anaerobically in bicarbonate minimal medium using 2-phenylethylamine (2-PEA), benzylamine (BAm), or 1-butylamine (1 mM each) as sole carbon and energy sources and nitrate (4 mM) as the electron acceptor. Growth with other substrates was described previously (16, 20). The cultures were incubated at 28°C in stoppered glass bottles without continuous shaking (volume, 0.1 to 2 liters) and discontinuously refed at the same concentrations upon substrate depletion. Growth was followed by determining the increase in optical density at 578 nm and the consumption of nitrate (Quantofix; Macherey-Nagel, Düren, Germany). The standard culture medium for *A. aromaticum* EbN1 contained 150 nM Na_2MoO_4 and 18 nM Na_2WO_4 of the highest purities available (99.9% and 99.995%, respectively). Tungstate-free medium was prepared in bottles with ultrapure water (conductivity, $<$0.05 μS/cm).

Preparation of cell extracts. All steps performed with cells or extracts of *A. aromaticum* EbN1 were carried out under strictly anoxic conditions. Cells were harvested by centrifugation at 17,000 $\times$ *g* and 4°C for 20 min (0.1- to 1-liter scale cultures). Sedimented cells were immediately frozen and stored at −80°C. For preparation of extracts, cells were suspended in one volume of 50 mM HEPPS {3-[4-(2-hydroxyethyl) piperazin-1-yl]propane-1-sulfonic acid}-KOH buffer (pH 8.0) or in the respective buffer for subsequent chromatographic enzyme enrichment (see below) containing 10% glycerol and 0.05 mg DNase I per ml. Cell suspensions were disrupted by sonication or passed thrice through a French pressure cell press. Cell debris and membranes were removed by ultracentrifugation at 100,000 $\times$ *g* and 4°C for 1 h. Supernatants (cell extract) were stored with 10% (vol/vol) glycerol at −80°C until use.

Enzyme activity assays. Enzyme activities involved in anaerobic degradation of phenylalanine were assayed photometrically in extracts of *A. aromaticum* EbN1 cells as described previously (20). These enzymes were aldehyde oxidoreductase (AOR), phenylacetaldehyde dehydrogenase (PDH), and phenylglyoxylate:acceptor oxidoreductase (PGOR). All assays were carried out with cell extracts at 25°C and were repeated at least twice.

Aminotransferase and amine dehydrogenase. Cell extracts of *A. aromaticum* were tested for aminotransferase and amine dehydrogenase activities in 100 mM potassium phosphate buffer, pH 7.8, testing 5 to 20 μl of cell extract in a volume of 1 ml. To identify putative 2-PEA- or BAm-aminotransferase activities, assays were set up in the presence and absence of 2 mM 2-oxoglutarate and tested for enhanced oxidation of the generated aromatic aldehydes in the presence of 2-oxoglutarate, using either NAD (1 mM; measured at 365 nm), potassium ferricyanide (up to 0.5 mM; measured at 420 nm), or ferricenium tetrafluoroborate (200 μM; measured at 290 nm) as the electron acceptor. Amine dehydrogenase activities were assayed in 50 mM Tris-HCl buffer, pH 8.4, using 80 μM dichloroindophenol (DCIP) plus 200 μM phenazine methosulphate (PMS) as electron acceptors (measured at 600 nm; ε = 21,000 M^{-1} cm^{-1}). Higher PMS concentrations did not lead to higher activity. Alternatively, the assay was also performed with 0.1 to 0.2 mM ferricenium tetrafluoroborate (measured at 290 nm), 0.2 to 0.5 mM potassium ferricyanide (measured at 420 nm), or 0.1 mM horse heart cytochrome *c* (measured at 550 nm) as electron acceptors. All assays were started by addition of 2 mM substrate (2-PEA or BAm).

Amine oxidase. Amine oxidation by molecular oxygen was assayed by measuring the production of either H_2O_2 from O_2 or the corresponding aldehyde from the amine. Production of H_2O_2 was measured by coupling the amine oxidation to horseradish peroxidase (HRP). The amine dehydrogenase assay mixture without added electron acceptors was mixed with HRP (5 μg ml^{-1}) and 250 μM ABTS, and the reaction was recorded at 405 nm (ε = 36.8 mM^{-1} cm^{-1}). The functionality of HRP was tested by addition of 50 μM H_2O_2 in each buffer system used (50 mM HEPPS-KOH, pH 8.5, Tris-HCl, pH 8.4, or potassium phosphate, pH 7.5). Alternatively, the reaction was assayed by the production of phenylacetaldehyde (PAld) from 2-PEA by coupling the reaction with the PAld-specific phenylacetaldehyde dehydrogenase (PDH) from *A. aromaticum*, which has been purified after recombinant expression in *Escherichia coli* (22).

AOR. The benzylviologen-dependent oxidation of PAld (AOR activity) was assayed under anoxic conditions as described previously (43) but using 100 mM Tris-HCl buffer (pH 8.4). The reaction was

started by the addition of PAld (2 mM) and recorded at 600 nm to measure reduction of benzylviologen (ε = 7,400 M^{-1} cm^{-1}).

PDH. The NAD- or NADP-dependent oxidation of phenylacetaldehyde was measured as described previously (44) but modified as follows. The enzyme was assayed in HEPPS-KOH buffer (pH 8.5) containing 1 mM NAD or NADP, and the reaction was started by addition of a low concentration of the substrate PAld (25 μM) because of the observed inhibition by higher concentrations of PAld (22). The absorbance was recorded at 365 nm (ε = 3,400 M^{-1} cm^{-1}).

BAld-DH. BAld-DH activities were measured as described for PDH activity. The assays coupled to NADP were performed with 1 mM BAld and those coupled to NAD with 50 μM BAld due to an observed substrate inhibition.

Phenylglyoxylate:acceptor oxidoreductase (PadEFGHI). Benzylviologen- and coenzyme A-dependent oxidation of phenylglyoxylate was assayed under anoxic conditions as described previously (45). The reaction was recorded at 600 nm by the increase of absorbance of reduced benzylviologen.

Purification of amine dehydrogenase isoenzymes. 2-PEA dehydrogenase (2-PEADH) activity was enriched from the *A. aromaticum* strain SR7_Δ*pdh* (20) grown anaerobically with 2-PEA in minimal medium. Twenty grams of wet cell mass was suspended in buffer A (20 mM Tris-HCl [pH 6.2], 10% glycerol) and disrupted with a French press cell, and, after ultracentrifugation (1 h, 100,000 × *g*, 4°C), the soluble cell extract was used for two subsequent chromatographic separations using an Äkta Pure fast protein liquid chromatography (GE Healthcare) system. Cell extract was first loaded onto an anion exchange column (DEAE-Sepharose 26/12) equilibrated with buffer A and eluted by a linear gradient of increasing NaCl concentration using buffer B (buffer A with 1 M NaCl). The 2-PEA oxidizing activity eluted at approximately 200 mM NaCl. The most active fractions were combined and rebuffered to buffer C (5 mM MES-KOH [pH 6.8], 1 mM potassium phosphate) using a HiPrep_26/10 desalting column (GE Healthcare) and applied to a hydroxyapatite column (CHT-I) equilibrated with buffer C. The column was developed with a linear gradient of increasing potassium phosphate concentrations (employing buffer D: 5 mM MES-KOH [pH 6.8], 400 mM potassium phosphate), and the enzyme eluted as a single peak at 70 mM potassium phosphate. Benzylamine dehydrogenase (BAmDH) activity was purified from a culture of *A. aromaticum* EbN1 grown anaerobically with BAm (7.2 g cell wet mass). The same protocol as that for enrichment of 2-PEA dehydrogenase was used, with BAmDH activity eluting differently: most of the enzyme already eluted in the flowthrough of the DEAE-Sepharose column, and in the second separation on hydroxyapatite, BAmDH eluted as a single peak when 130 mM potassium phosphate was applied. Active fractions were supplied with 10% (vol/vol) glycerol and used either immediately for further processing or stored anoxically at −80°C until further use.

Phylogenetic analysis. The amino acid sequences of amine dehydrogenases were analyzed by BLAST searches against the NCBI database using default settings. Alignment of selected sequences was performed by Clustal Omega (https://www.ebi.ac.uk/Tools/msa/clustalo/) (46), and phylogenetic trees were constructed by iTol (https://itol.embl.de/) (47).

Other methods. Protein concentration was determined by the method of Bradford (48) using bovine serum albumin as the standard protein. Heme staining was prepared as described preciously (49). The UV-Vis spectra of 2-PEADH and BAmDH were recorded on a Cary 60 spectrophotometer (Agilent, Waldbronn, Germany). Purified enzyme was measured as isolated and after incubation with the corresponding substrates or dithionite. Proteins were separated by discontinuous SDS-PAGE and stained by Coomassie blue (50). Molecular masses of proteins were estimated by Ferguson plot analysis, using nondenaturing gel electrophoresis with polyacrylamide concentrations of 6, 7, 8, and 10% (51). Standards were bovine serum albumin and its oligomers (67 to 268 kDa) and ovalbumin (45 kDa). The identities of proteins separated by SDS-PAGE were determined by mass spectrometry using a 4800 Proteomics Analyzer (MDS Sciex, Concord, ON, Canada). Mass spectrometry data were evaluated against an in-house database using Mascot embedded into GPS explorer software (MDS Sciex, Concord, ON, Canada). The retrieved sequences represented the first or only hits and showed convincing statistical parameters (peptide counts of >28 with score values of >1,000 for GenBank accession numbers CAI07356 and CAI07353 of 2-PEADH and peptide counts of >230 with score values of >70,000 for CAI09065 and CAI09068 of BAmDH).

ACKNOWLEDGMENTS

We thank Iris Schall for technical assistance.

This work was supported by grants from the Deutsche Forschungsgemeinschaft (priority program 1927) and the SYNMIKRO LOEWE Center, Marburg.

REFERENCES

1. Hacisalihoglu A, Jongejan JA, Duine JA. 1997. Distribution of amine oxidases and amine dehydrogenases in bacteria grown on primary amines and characterization of the amine oxidase from *Klebsiella oxytoca*. Microbiology 143:505–512. https://doi.org/10.1099/00221287-143-2-505.
2. Murooka Y, Doi N, Harada T. 1979. Distribution of membrane-bound monoamine oxidase in bacteria. Appl Environ Microbiol 38:565–569.
3. Iwaki M, Yagi T, Horiike K, Saeki Y, Ushijima T, Nozaki M. 1983. Crystallization and properties of aromatic amine dehydrogenase from *Pseudomonas* sp. Arch Biochem Biophys 220:253–262. https://doi.org/10.1016/0003-9861(83)90408-3.
4. Govindaraj S, Eisenstein E, Jones LH, Sanders-Loehr J, Chistoserdov AY, Davidson VL, Edwards SL. 1994. Aromatic amine dehydrogenase, a second tryptophan tryptophylquinone enzyme. J Bacteriol 176:2922–2929. https://doi.org/10.1128/jb.176.10.2922-2929.1994.
5. de Beer R, Duine JA, Frank J, Large PJ. 1980. The prosthetic group of methylamine dehydrogenase from *Pseudomonas* AM1: evidence for a

quinone structure. Biochim Biophys Acta 622:370–374. https://doi.org/10.1016/0005-2795(80)90050-1.
6. Duine JA, Frank J, Verwiel PE. 1980. Structure and activity of the prosthetic group of methanol dehydrogenase. Eur J Biochem 108:187–192. https://doi.org/10.1111/j.1432-1033.1980.tb04711.x.
7. Ghosh M, Anthony C, Harlos K, Goodwin MG, Blake C. 1995. The refined structure of the quinoprotein methanol dehydrogenase from *Methylobacterium extorquens* at 1.94 Å. Structure 3:177–187. https://doi.org/10.1016/S0969-2126(01)00148-4.
8. Duine JA. 1991. Quinoproteins: enzymes containing the quinonoid cofactor pyrroloquinoline quinone, topaquinone or tryptophyl-tryptophan quinone. Eur J Biochem 200:271–284. https://doi.org/10.1111/j.1432-1033.1991.tb16183.x.
9. Davidson VL. 2005. Structure and mechanism of tryptophylquinone enzymes. Bioorg Chem 33:159–170. https://doi.org/10.1016/j.bioorg.2004.10.001.
10. Duine JA. 2001. Cofactor diversity in biological oxidations: implications and applications. Chem Rec 1:74–83. https://doi.org/10.1002/1528-0691(2001)1:1<74::AID-TCR10>3.0.CO;2-E.
11. Klinman JP, Bonnot F. 2014. Intrigues and intricacies of the biosynthetic pathways for the enzymatic quinocofactors: PQQ, TTQ, CTQ, TPQ, and LTQ. Chem Rev 114:4343–4365. https://doi.org/10.1021/cr400475g.
12. Adachi O, Kubota T, Hacisalihoglu A, Toyama H, Shinagawa E, Duine JA, Matsushita K. 1998. Characterization of quinohemoprotein amine dehydrogenase from *Pseudomonas putida*. Biosci Biotechnol Biochem 62:469–478. https://doi.org/10.1271/bbb.62.469.
13. Takagi K, Torimura M, Kawaguchi K, Kano K, Ikeda T. 1999. Biochemical and electrochemical characterization of quinohemoprotein amine dehydrogenase from *Paracoccus denitrificans*. Biochemistry 25:6935–6942. https://doi.org/10.1021/bi9828268.
14. Rigby SE, Basran J, Combe JP, Mohsen AW, Toogood H, van Thiel A, Sutcliffe MJ, Leys D, Munro AW, Scrutton NS. 2005. Flavoenzyme catalysed oxidation of amines: roles for flavin and protein-based radicals. Biochem Soc Trans 33:754–757. https://doi.org/10.1042/BST0330754.
15. Nakai T, Deguchi T, Frébort I, Tanizawa K, Okajima T. 2014. Identification of genes essential for the biogenesis of quinohemoprotein amine dehydrogenase. Biochemistry 53:895–907. https://doi.org/10.1021/bi401625m.
16. Rabus R, Widdel F. 1995. Anaerobic degradation of ethylbenzene and other aromatic hydrocarbons by new denitrifying bacteria. Arch Microbiol 163:96–103. https://doi.org/10.1007/BF00381782.
17. Wöhlbrand L, Kallerhoff B, Lange D, Hufnagel P, Thiermann J, Reinhardt R, Rabus R. 2007. Functional proteomic view of metabolic regulation in "*Aromatoleum aromaticum*" strain EbN1. Proteomics 7:2222–2239. https://doi.org/10.1002/pmic.200600987.
18. Rabus R, Wöhlbrand L, Thies D, Meyer M, Reinhold-Hurek B, Kämpfer P. 2019. *Aromatoleum* gen. nov., a novel genus accommodating the phylogenetic lineage including *Azoarcus evansii* and related species, and proposal of *Aromatoleum aromaticum* sp. nov., *Aromatoleum petrolei* sp. nov., *Aromatoleum bremense* sp. nov., *Aromatoleum toluolicum* sp. nov. and *Aromatoleum diolicum* sp. nov. Int J Syst Evol Microbiol 69:982–997. https://doi.org/10.1099/ijsem.0.003244.
19. Fuchs G, Boll M, Heider J. 2011. Microbial degradation of aromatic compounds from one strategy to four. Nat Rev Microbiol 9:803–816. https://doi.org/10.1038/nrmicro2652.
20. Schmitt G, Arndt F, Kahnt J, Heider J. 2017. Adaptations to a loss-of-function mutation in the betaproteobacterium *Aromatoleum aromaticum*: recruitment of alternative enzymes for anaerobic phenylalanine degradation. J Bacteriol 199:e00383-17. https://doi.org/10.1128/JB.00383-17.
21. Rabus R, Kube M, Heider J, Beck A, Heitmann K, Widdel F, Reinhardt R. 2005. The genome sequence of an anaerobic aromatic-degrading denitrifying bacterium, strain EbN1. Arch Microbiol 183:27–36. https://doi.org/10.1007/s00203-004-0742-9.
22. Debnar-Daumler C, Seubert A, Schmitt G, Heider J. 2014. Simultaneous involvement of a tungsten-containing aldehyde:ferredoxin oxidoreductase and a phenylacetaldehyde dehydrogenase in anaerobic phenylalanine metabolism. J Bacteriol 196:483–492. https://doi.org/10.1128/JB.00980-13.
23. Arndt F, Schmitt G, Winiarska A, Saft M, Seubert A, Kahnt J, Heider J. 2019. Characterization of an aldehyde oxidoreductase from the mesophilic bacterium Aromatoleum aromaticum EbN1, a member of a new subfamily of tungsten-containing enzymes. Front Microbiol 10:71. https://doi.org/10.3389/fmicb.2019.00071.
24. Heider J, Fuchs G. 1997. Anaerobic metabolism of aromatic compounds. Eur J Biochem 243:577–596. https://doi.org/10.1111/j.1432-1033.1997.00577.x.
25. Ono K, Okajima T, Tani M, Kuroda S, Sun D, Davidson VL, Tanizawa K. 2006. Involvement of a putative [Fe-S]-cluster-binding protein in the biogenesis of quinohemoprotein amine dehydrogenase. J Biol Chem 281:13672–13684. https://doi.org/10.1074/jbc.M600029200.
26. Nakai T, Ono K, Kuroda S, Tanizawa K, Okajima T. 2012. An unusual subtilisin-like serine protease is essential for biogenesis of quinohemoprotein amine dehydrogenase. J Biol Chem 287:6530–6538. https://doi.org/10.1074/jbc.M111.324756.
27. Datta S, Mori Y, Takagi K, Kawaguchi K, Chen ZW, Okajima T, Kuroda S, Ikeda T, Kano K, Tanizawa K, Mathews FS. 2001. Structure of a quinohemoprotein amine dehydrogenase with an uncommon redox cofactor and highly unusual crosslinking. Proc Natl Acad Sci U S A 98:14268–14273. https://doi.org/10.1073/pnas.241429098.
28. Satoh A, Kim JK, Miyahara I, Devreese B, Vandenberghe I, Hacisalihoglu A, Okajima T, Kuroda S, Adachi O, Duine JA, Van Beeumen J, Tanizawa K, Hirotsu K. 2002. Crystal structure of quinohemoprotein amine dehydrogenase from *Pseudomonas putida*. Identification of a novel quinone cofactor encaged by multiple thioether cross-bridges. J Biol Chem 277:2830–2834. https://doi.org/10.1074/jbc.M109090200.
29. Nakai T, Ito H, Kobayashi K, Takahashi Y, Hori H, Tsubaki M, Tanizawa K, Okajima T. 2015. The radical S-adenosyl-L-methionine enzyme QhpD catalyzes sequential formation of intra-protein sulfur-to-methylene carbon thioether bonds. J Biol Chem 290:11144–11166. https://doi.org/10.1074/jbc.M115.638320.
30. Vandenberghe I, Kim JK, Devreese B, Hacisalihoglu A, Iwabuki H, Okajima T, Kuroda S, Adachi O, Jongejan JA, Duine JA, Tanizawa K, Van Beeumen J. 2001. The covalent structure of the small subunit from *Pseudomonas putida* amine dehydrogenase reveals the presence of three novel types of internal cross-linkages, all involving cysteine in a thioether bond. J Biol Chem 276:42923–42931. https://doi.org/10.1074/jbc.M107164200.
31. Fujieda N, Mori M, Kano K, Ikeda T. 2003. Redox properties of quinohemoprotein amine dehydrogenase from *Paracoccus denitrificans*. Biochim Biophys Acta 1647:289–296. https://doi.org/10.1016/S1570-9639(03)00072-4.
32. Garber E, Margoliash E. 1994. Circular dichroism studies of the binding of mammalian and non-mammalian cytochromes *c* to cytochrome *c* oxidase, cytochrome *c* peroxidase, and polyanions. Biochim Biophys Acta 1187:289–295. https://doi.org/10.1016/0005-2728(94)90002-7.
33. Shinagawa E, Matsushita K, Nakashima K, Adachi O, Ameyama M. 1988. Crystallization and properties of amine dehydrogenase from *Pseudomonas* sp. Agric Biol Chem 52:2255–2263. https://doi.org/10.1080/00021369.1988.10869019.
34. Takagi K, Yamamoto K, Kano K, Ikeda T. 2001. New pathway of amine oxidation respiratory chain of *Paracoccus denitrificans* IFO 12442. Eur J Biochem 268:470–476. https://doi.org/10.1046/j.1432-1033.2001.01912.x.
35. Durham DR, Perry JJ. 1978. Purification and characterization of a heme-containing amine dehydrogenase from *Pseudomonas putida*. J Bacteriol 134:837–843.
36. Jiménez JI, Miñambres B, García JL, Díaz E. 2002. Genomic analysis of the aromatic catabolic pathways from Pseudomonas putida KT2440. Environ Microbiol 4:824–841. https://doi.org/10.1046/j.1462-2920.2002.00370.x.
37. Sun D, Ono K, Okajima T, Tanizawa K, Uchida M, Yamamoto Y, Mathews FS, Davidson VL. 2003. Chemical and kinetic reaction mechanisms of quinohemoprotein amine dehydrogenase from *Paracoccus denitrificans*. Biochemistry 42:10896–10903. https://doi.org/10.1021/bi035062r.
38. Shen XH, Zhou NY, Liu SJ. 2012. Degradation and assimilation of aromatic compounds by *Corynebacterium glutamicum*: another potential for applications for this bacterium? Appl Microbiol Biotechnol 95:77–89. https://doi.org/10.1007/s00253-012-4139-4.
39. Zeng J, Spiro S. 2013. Finely tuned regulation of the aromatic amine degradation pathway in *Escherichia coli*. J Bacteriol 195:5141–5150. https://doi.org/10.1128/JB.00837-13.
40. Martín-Moldes Z, Zamarro MT, Del Cerro C, Valencia A, Gómez MJ, Arcas A, Udaondo Z, García JL, Nogales J, Carmona M, Díaz E. 2015. Whole-genome analysis of *Azoarcus* sp. strain CIB provides genetic insights to its different lifestyles and predicts novel metabolic features. Syst Appl Microbiol 38:462–471. https://doi.org/10.1016/j.syapm.2015.07.002.
41. Pearce DA, Page MD, Norris HAC, Tomlinson EJ, Stuart J, Ferguson SJ. 1998. Identification of the contiguous *Paracoccus denitrificans ccmF* and *ccmH* genes: disruption of *ccmF*, encoding a putative transporter, results in formation of an unstable apocytochrome *c* and deficiency in sidero-

phore production. Microbiology 144:467–477. https://doi.org/10.1099/00221287-144-2-467.
42. Wöhlbrand L, Rabus R. 2009. Development of a genetic system for the denitrifying bacterium "*Aromatoleum aromaticum*" strain EbN1. J Mol Microbiol Biotechnol 17:41–52. https://doi.org/10.1159/000159194.
43. Heider J, Ma K, Adams M. 1995. Purification, characterization, and metabolic function of tungsten-containing aldehyde ferredoxin oxidoreductase from the hyperthermophilic and proteolytic archaeon *Thermococcus* strain ES-1. J Bacteriol 177:4757–4764. https://doi.org/10.1128/jb.177.16.4757-4764.1995.
44. Schneider S, Mohamed M-S, Fuchs G. 1997. Anaerobic metabolism of L-phenylalanine via benzoyl-CoA in the denitrifying bacterium *Thauera aromatica*. Arch Microbiol 168:310–320. https://doi.org/10.1007/s002030050504.
45. Hirsch W, Schägger H, Fuchs G. 1998. Phenylglyoxylate:NAD^+ oxidoreductase (CoA benzoylating), a new enzyme of anaerobic phenylalanine metabolism in the denitrifying bacterium *Azoarcus evansii*. Eur J Biochem 251:907–915. https://doi.org/10.1046/j.1432-1327.1998.2510907.x.
46. Sievers F, Wilm A, Dineen D, Gibson TJ, Karplus K, Li W, Lopez R, McWilliam H, Remmert M, Söding J, Thompson JD, Higgins DG. 2014. Fast, scalable generation of high-quality protein multiple sequence alignments using Clustal Omega. Mol Syst Biol 7:539. https://doi.org/10.1038/msb.2011.75.
47. Letunic I, Bork P. 2007. Interactive Tree Of Life (iTOL): an online tool for phylogenetic tree display and annotation. Bioinformatics 23:127–128. https://doi.org/10.1093/bioinformatics/btl529.
48. Bradford MM. 1976. A rapid and sensitive method for the quantitation of microgram quantities of protein utilizing the principle of protein-dye binding. Anal Biochem 72:248–254. https://doi.org/10.1016/0003-2697(76)90527-3.
49. Goodhew CF, Brown KR, Pettigrew GW. 1986. Haem staining in gels, a useful tool in the study of bacterial *c*-type cytochromes. Biochim Biophys Acta 852:288–294. https://doi.org/10.1016/0005-2728(86)90234-3.
50. Laemmli V. 1970. Determination of protein molecular weight in polyacrylamide gels. Nature 227:680–685. https://doi.org/10.1038/227680a0.
51. Coligan JE, Dunn BM, Ploegh HE, Speicher DW, Wingfield PT. 2004. Current protocols in protein science. John Wiley & Sons, New York, NY. https://doi.org/10.1002/prot.340240303.